



OPEN

Age-associated B cells are long-lasting effectors that impede latent γ HV68 reactivation

Isobel C. Mouat^{1,2}, Iryna Shanina² & Marc S. Horwitz^{2,3}✉

Age-associated B cells (ABCs; CD19⁺CD11c⁺T-bet⁺) are a unique population that are increased in an array of viral infections, though their role during latent infection is largely unexplored. Here, we use murine gammaherpesvirus 68 (γ HV68) to demonstrate that ABCs remain elevated long-term during latent infection and express IFN γ and TNF. Using a recombinant γ HV68 that is cleared following acute infection, we show that ABCs persist in the absence of latent virus, though their expression of IFN γ and TNF is decreased. With a fluorescent reporter gene-expressing γ HV68 we demonstrate that ABCs are infected with γ HV68 at similar rates to other previously activated B cells. We find that mice without ABCs display defects in anti-viral IgG2a/c antibodies and are more susceptible to reactivation of γ HV68 following virus challenges that typically do not break latency. Together, these results indicate that ABCs are a persistent effector subset during latent viral infection that impedes γ HV68 reactivation.

Humans are infected with an array of herpesviruses that persist within us throughout our lives and require continuous surveillance by the host immune system. Gammaherpesvirus-68 (γ HV68) is a murine model of human gamma herpesviruses Epstein-Barr virus and Kaposi sarcoma-associated herpesvirus¹. γ HV68, like other herpesviruses, deploys distinct transcriptional programs during lytic and latent infection, each of which requires a distinct immune response². Age-associated B cells (ABCs) are a unique B cell population implicated in viral infection, autoimmunity, and aging^{3–6}. ABCs (CD19⁺CD11c⁺T-bet⁺) are induced following γ HV68 infection⁷, though their function throughout the course of infection is not clear. In this study we examine the response of and role for ABCs throughout γ HV68 infection, from acute infection through long-term latency.

ABCs were identified in 2011 in the context of female aging and autoimmunity^{3,4} and have since been shown to be increased in an array of viral infections including lymphocytic choriomeningitis virus (LCMV), murine cytomegalovirus, γ HV68, vaccinia, human immunodeficiency virus, rhinovirus, SARS-CoV2, and influenza^{7–12}. ABCs are elevated in the spleen and circulation during active viral infections and persist primarily in the spleen during chronic infection or upon infection resolution^{9,10}. ABCs display multiple functional capacities including the secretion of antibodies, anti-viral cytokines and the activation of T cells^{13,14}. T-bet expression in B cells is required for IgG2a/c class switching¹⁵ and lack of ABCs exacerbates LCMV chronic infection in mice¹⁶. We predict that ABCs could be playing a role throughout γ HV68 infection due to their long-term persistence, activation of T cells, and continuous cytokine and antibody production.

Lytic γ HV68 infection is primarily cleared by CD8⁺ T cells^{17,18}, following which γ HV68 persists in a latent state mainly in previously activated B cells¹⁹. During latency the immune response persists even though there is minimal production of viral genes and limited production of new virions²⁰. Both humoral and cellular responses contribute to controlling γ HV68 infection long-term^{21,22}. Mice lacking either antibodies or T cells are both able to control γ HV68 latency, though mice lacking both antibodies and T cells display elevated γ HV68 reactivation^{21,23}. IFN γ is critical for controlling γ HV68 replication and reactivation from latency^{24,25}.

B cells are also known to be important during latent γ HV68 infection. B cells act as the primary latent viral reservoir, are required for movement from the lung to the spleen at the onset of latency, and mice deficient in B cells are unable to develop latency following intranasal infection^{19,26–28}. B cells secrete anti-viral antibodies long term²⁹, but also may inhibit reactivation via secretion of anti-viral cytokines or help to virus-specific T cells. The precise B cell subsets, mechanisms, and factors that facilitate the maintenance of latency and prevent reactivation are not fully understood.

¹Centre for Inflammation Research, University of Edinburgh, Edinburgh, UK. ²Department of Microbiology and Immunology, The University of British Columbia, Vancouver, BC, Canada. ³Life Sciences Centre, University of British Columbia, Room 3551, 2350 Health Sciences Mall, Vancouver, BC V6T 1Z3, Canada. ✉email: mhorwitz@mail.ubc.ca

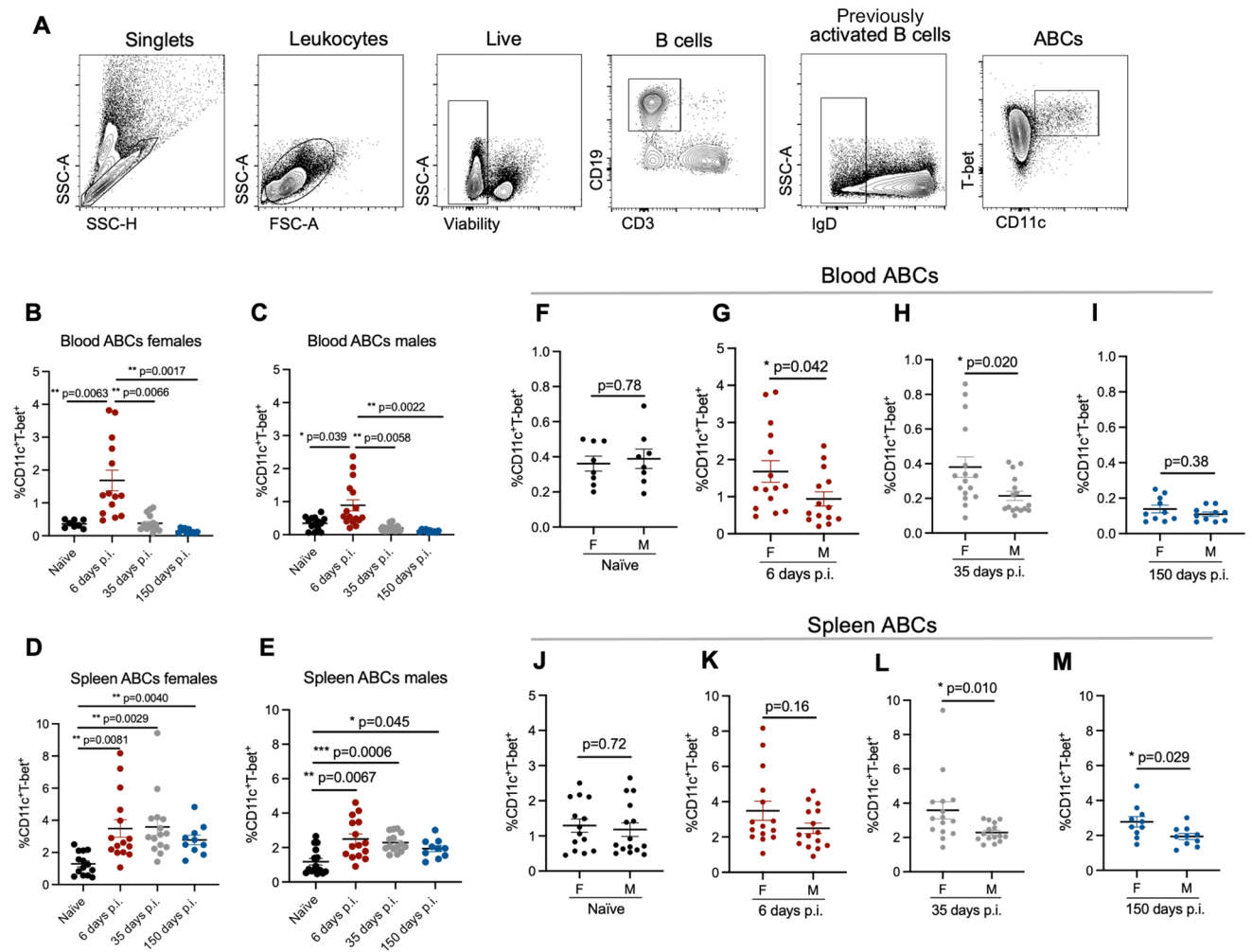


Figure 1. ABCs expand in the blood and spleen throughout γ HV68 infection. Blood and spleen collected from C57BL/6(J) mice (6–8-week-old at infection) mock-infected with media (naïve, black circles) or infected i.p. with γ HV68 for 6 (red circles), 35 (grey circles), or 150 (blue circles) days and processed for flow cytometry. **(A)** Representative gating strategy of ABCs. IgD, CD11c, and T-bet gating used fluorescence-minus-one (FMO) controls. **(B–E)** Proportion of ABCs (CD11c⁺T-bet⁺) of previously activated B cells (CD19⁺IgD⁻) in the blood and spleen of male and female mice. **(F–I)** Proportion of ABCs (CD11c⁺T-bet⁺) of previously activated B cells (CD19⁺IgD⁻) in the blood or spleen of male and female mice. Same data as presented in panels **(B–E)**. n = 10–15 mice per group, data compiled from 4 experiments. Each data point represents an individual mouse. Data presented as mean \pm SEM. Analyzed by **(B–E)** one-way ANOVA or **(F–M)** Mann–Whitney test. p-values indicated as asterix as follows: ***p < 0.001, **p < 0.01, *p < 0.05.

The role of ABCs during acute and latent herpesvirus infection is unknown. Herein, using various tools, we investigate the relationship between γ HV68 and ABCs throughout lytic and latent infection. We find that ABCs expand during acute γ HV68 infection and persist in the spleen during latency. Well after the initial establishment of latency, ABCs continuously secrete anti-viral cytokines and antibodies and in the face of heterologous challenge, ABCs are required to restrain latent γ HV68 reactivation. Thus, our findings highlight a novel role for ABCs as effector cells during γ HV68 latency.

Results

ABCs are induced and maintained following γ HV68 infection in a sex-biased manner. To examine the relative proportion of ABCs during acute and latent γ HV68 infection, C57BL/6(J) mice were mock-infected with media (naïve) or infected with γ HV68 for 6, 35, and 150 days, blood and spleen were collected and analyzed by flow cytometry to measure ABCs. A gating scheme, described in Fig. 1A, identified CD11c⁺T-bet⁺ as a proportion of previously activated B cells (CD19⁺IgD⁻). We observed the relative proportion of ABCs increased in circulation during acute γ HV68 infection (6 days p.i.) compared to naïve mice (Fig. 1B,C). Once latency was well established (day 35 and 150 p.i.), the proportion of circulating ABCs decreased to pre-infection levels (Fig. 1B,C). This indicates that ABCs circulate in response to the lytic γ HV68 infection but do not remain elevated in circulation during latency. In the spleen, the relative proportion and total number of ABCs was increased during acute γ HV68 infection (day 6 p.i.) relative to naïve mice and remained elevated during latent

γ HV68 infection at 35 days p.i. and 150 days p.i. (Fig. 1D,E, Fig. S1). These results support previous findings that the spleen is a major site for ABCs following the clearance of acute viral infection¹⁰.

Intriguingly, we observed that the proportion of ABCs is increased in females as compared to males in both the blood and spleen throughout infection (Fig. 1F–M). Previously, we demonstrated that ABCs display a sex bias during experimental autoimmune encephalomyelitis and at 35 days post- γ HV68 infection in the spleen³⁰. Here, we have extended this finding and shown that ABCs display female sex bias in both the circulation and spleen during lytic and latent γ HV68 infection. While ABCs increase in both females and males following γ HV68 infection, there is a sex bias leading to greater expansion in females. These results demonstrate that ABCs are increased in circulation during acute γ HV68 infection and continue to endure in the spleen long-term during latent infection.

ABCs express anti-viral cytokines in response to latent γ HV68 infection. To begin investigating the role of ABCs in the anti-viral response, we measured ABC expression of anti-viral cytokines interferon- γ (IFN γ) and tumor necrosis factor- α (TNF) in the spleen at 6, 35, and 150 days p.i. We found that during acute γ HV68 infection (6 days p.i.), roughly 40% of ABCs in the spleen expressed IFN γ and TNF, as compared to about 10% of ABCs in naïve mice (Fig. 2A,B). During latent infection (35 days and 150 days p.i.), a significantly increased proportion of ABCs continued to express IFN γ and TNF compared to naïve mice, though the proportion of ABCs expressing IFN γ and TNF was decreased compared to acute infection (Fig. 2A,B). Throughout the acute and latent infection, we observed a downregulation of IL-17A expression on ABCs (Fig. 2C).

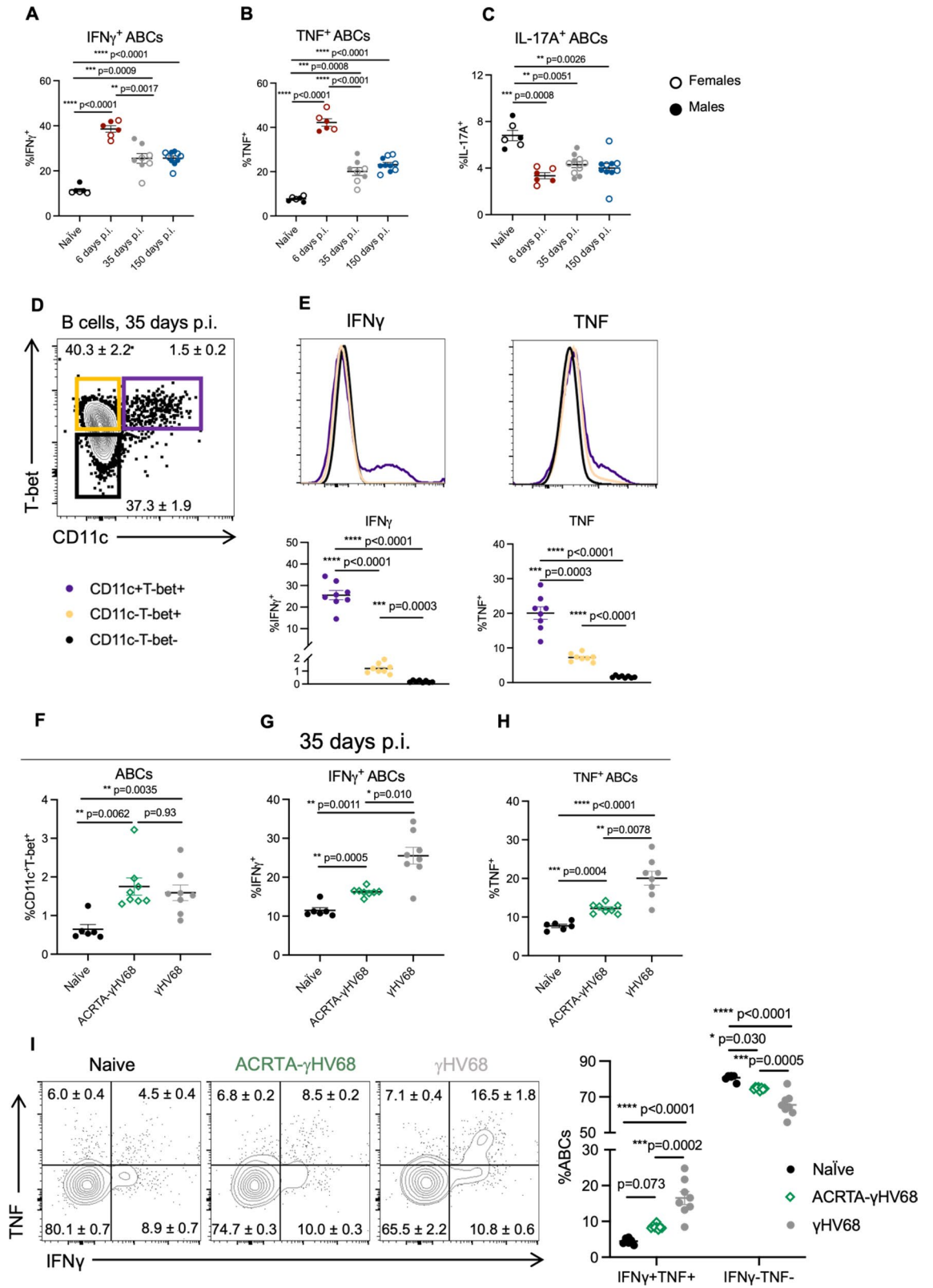
To determine if the level of cytokine expression was distinct from other B cells, we compared the proportion of ABCs expressing IFN γ and TNF to non-ABC B cells. Specifically, we examined expression on ABCs compared to CD11c⁻Tbet⁺ and CD11c⁻Tbet⁻ B cells 35 days post- γ HV68 infection (Fig. 2D). A significantly increased proportion of ABCs expressed IFN γ and TNF compared to non-ABC B cells, both CD11c⁻Tbet⁺ and CD11c⁻Tbet⁻ B cells, in the spleen (Fig. 2E). The mean fluorescent intensity (MFI) of IFN γ and TNF, of IFN γ or TNF positive cells, was significantly increased on ABCs compared to both non-ABC populations (Fig. S2A,B). CD11c⁻Tbet⁺ B cells expressed an intermediate level of IFN γ and TNF between ABCs and CD11c⁻Tbet⁻ B cells (Fig. 2E, Fig. S2A,B). Sex differences in ABC cytokine expression were not observed (Fig. 2A–C, Fig. S3A–C). The high level of IFN γ and TNF cytokine expression indicates that ABCs may be functioning in a unique anti-viral capacity during latent infection.

To explore the relationship between latent γ HV68 and the ABC population, we infected mice with ACRTA- γ HV68, a recombinant strain of γ HV68 in which the genes responsible for latency are deleted and a lytic gene, RTA, is constitutively expressed³¹. As a result, γ HV68 infection is cleared following acute infection without ever establishing latency. We found that, at 35 days p.i., a time point at which ACRTA- γ HV68 is cleared, ABCs are increased to the same level in the spleens of ACRTA- γ HV68 infected mice as compared to spleens in mice infected with WT γ HV68 (Fig. 2F). Thus, ABCs persist in the absence of latent virus, in a manner similar to memory cells that remain following acute infection.

While the proportion of ABCs remained elevated in the absence of latent virus, cytokine expression was altered. The proportion of ABCs in ACRTA- γ HV68-infected mice expressing IFN γ and TNF at 35 days p.i. was significantly reduced compared to those infected with WT γ HV68 while remaining significantly elevated compared to naïve mice (Fig. 2G,H). Additionally, the IFN γ ⁺ ABCs in mice infected with ACRTA- γ HV68 displayed a lower MFI than those from γ HV68-infected mice, though the TNF MFI was not significantly different between the two groups (Fig. S2C,D). Without the presence of the latent virus, we observe a decrease specifically in the proportion of ABCs that doubly express both IFN γ and TNF as well as an increase in ABCs that are negative for the expression of both IFN γ and TNF as compared to ABCs from WT γ HV68-infected mice (Fig. 2I). This finding indicates that ABCs respond to the latent virus by producing both IFN γ and TNF.

Together, these results show that ABCs are a predominant B cell subset expressing anti-viral cytokines IFN γ and TNF during latent γ HV68. Further, our data establish that high levels of expression of these cytokines are dependent on the presence of the latent virus. These findings suggest that ABCs recognize the presence of the quiescent latent virus and respond by expressing anti-viral cytokines.

ABCs are susceptible to γ HV68 infection but are not a major viral reservoir. γ HV68 is known to infect B cells, in particular germinal centre and memory B cells^{32–35}. To determine if ABCs are directly infected by γ HV68, we used a previously developed fluorescent strain of γ HV68, γ HV68.H2bYFP³⁶ where fluorescence is easily detectable during acute infection, but over time falls off during latent infection. Mice were infected with γ HV68.H2bYFP and 8 days p.i. spleens were collected, and flow cytometry was performed. We found that, during acute infection, a small proportion of ABCs were infected with γ HV68. The same proportion of ABCs were positive for the fluorescent virus ($1.2 \pm 0.3\%$) as observed in previously activated B cells ($1.1 \pm 0.2\%$, Fig. 3A,B), demonstrating that ABCs are not preferably targeted for infection. To our knowledge this is the first evidence of a virus directly infecting ABCs. We next asked what proportion of the γ HV68 reservoir is made up of ABCs. The primary reservoir for γ HV68 is previously activated B cells which aligns with our results that 73% of γ HV68-infected cells are IgD⁻ B cells (Fig. 3C). We found that ABCs make up only 6% of γ HV68-infected cells (Fig. 3C). Other infected cell populations included innate cells such as macrophages and DCs, in alignment with previous findings³², as well as a small proportion of NK and T cells (Fig. 3C). We also examined the relationship between infection of ABCs and expression of IFN γ . We observed that during acute infection the proportion of ABCs expressing IFN γ was significantly lower in ABCs infected with γ HV68 ($4.3 \pm 1.3\%$) as compared to uninfected ABCs ($32.2 \pm 1.0\%$, Fig. 3D). These results indicate that direct infection of ABCs was not driving IFN γ production and that at least during acute infection, ABCs are susceptible to virus-driven downregulation of IFN γ . These



◀Figure 2. Cytokine production by ABCs in the spleen during γ HV68 and ACRTA- γ HV68 infection. (A–C) C57BL/6(J) mice (6–8-week-old at infection) mock-infected with media (naïve) or infected i.p. with γ HV68 for 6, 35, or 150 days. Spleens collected and processed for flow cytometry. Proportion of ABCs in the spleen expressing (A) IFN γ , (B) TNF, or (C) IL-17A, with females presented as open circles and males as filled circles. (D) Gating of ABCs (CD11c⁺T-bet⁺) and non-ABC B cells (CD11c⁻T-bet⁺ and CD11c⁻T-bet⁻), previously gated on CD19⁺IgD⁻ cells in the spleen. (E) Representative histograms and dot plots of the proportion of ABCs and non-ABC B cells (CD11c⁻T-bet⁺ and CD11c⁻T-bet⁻) expressing IFN γ and TNF from mice infected with γ HV68 for 35 days. (F–H) C57BL/6(J) mice mock-infected with media (Naïve, black circles) or infected i.p. with γ HV68 (grey circles) or ACRTA- γ HV68 (green diamonds) for 35 days and spleens processed for flow cytometry. (F) Proportion of ABCs (CD11c⁺T-bet⁺) of previously activated B cells (CD19⁺IgD⁻) in the spleen. Proportion of ABCs (CD19⁺CD11c⁺T-bet⁺) in the spleen expressing (G) IFN γ or (H) TNF. (I) Representative plots and quantification of the proportion of ABCs expressing IFN γ and TNF. Equivalent numbers of females and males per group in all panels. (A–C) n = 6–10 mice per group, data combined from two experiments. (E–I) n = 6–8 mice per group, representative of two experiments. Each data point represents an individual mouse. Data presented as mean \pm SEM. Analyzed by one-way ANOVA. p-values indicated as asterisks as follows: ****p < 0.0001, ***p < 0.001, **p < 0.01, *p < 0.05.

findings demonstrate that although a portion of ABCs are infected with γ HV68, ABCs are not the major target for γ HV68.

ABCs are dispensable for the control of acute infection and establishment of latency. To further examine the role(s) of ABCs in γ HV68 infection, mice with a floxed B cell specific T-bet deletion were followed post-infection. Specifically, *Tbx21^{fl/fl}Cd19^{cre/+}* (KO) and littermate *Tbx21^{fl/fl}Cd19^{+/+}* (Ctrl) mice were infected with γ HV68 for 6 or 35 days and the spleen was collected to examine the quantity of γ HV68 by qPCR and the immune cell composition (Fig. 4A). Mice were genotyped by PCR and loss of ABCs in KO mice was confirmed by flow cytometry (Fig. 4B). No differences in clinical symptoms or weight changes were observed during γ HV68 infection between Ctrl or KO mice (Fig. S4A).

To determine if knocking out ABCs alters immune cell composition, Ctrl and KO mice were infected or mock-infected with γ HV68 and spleens analyzed at 6 or 35 days by flow cytometry to examine various T cell, B cell, and innate immune cell populations. No difference in the total number of splenocytes was observed (Fig. S4B). The composition of the splenic immune profile was similar between Ctrl and KO mice with no significant differences observed in the relative proportions of B cells, CD8 T cells, DCs, neutrophils, NK cells, or macrophages between mock-infected mice or those infected with γ HV68 for 6 or 35 days, though KO mice had greater proportions of CD4 T cells than Ctrl mice 35 days post-infection (Fig. S5).

We then measured the quantity of γ HV68 in the spleens of Ctrl and KO mice infected for 6 and 35 days by qPCR. We found no difference in that the quantity of γ HV68 at 6 and 35 days p.i. between Ctrl and KO mice (Fig. 4C,D) and the quantity of γ HV68 did not differ between male and female mice (Fig. S4C,D). To confirm that KO mice effectively control the lytic infection and develop latency, we infected Ctrl and KO mice with latency-deficient ACRTA- γ HV68 for 35 days. We found that KO mice, like Ctrl mice, displayed similar viral loads that were near or below the limit of detection when infected with ACRTA- γ HV68 (Fig. 4E). As no virus was detected at day 35, mice lacking ABCs were effectively controlling the lytic infection. Furthermore, we examined splenocytes from Ctrl and KO mice for the expression of genes associated with lytic infection (*Orf50*, *Orf68*) or latent infection (*Orf73*), and observed no differences in the relative expression of *Orf50*, *Orf68*, or *Orf73* between Ctrl and KO mice (Fig. 4F). *Orf50* encodes the replication and transcription activator protein, which initiates viral lytic gene expression³⁷. *Orf68* encodes a packaging protein that assists in moving the newly replicated viral genomes to the packaging motor, where they are loaded into capsids³⁸. *Orf73* encodes for the latency-associated nuclear antigen that is required for the establishment and maintenance of latent infection^{39,40}. As such, equal expression of lytic and latency-associated genes *Orf50*, *Orf68*, and *Orf73* between Ctrl and KO mice suggests the harboring of similar levels of lytic and latent γ HV68. Together, these results demonstrate that ABCs are not required for the clearance of acute infection and establishment of latency in steady-state conditions.

Lack of ABCs results in a dysregulated γ HV68 antibody response but does not alter the viral reservoir or anti-viral T cell response. ABCs are known to secrete anti-viral IgG2a/c⁷, and transfer of serum into mice without ABCs during LCMV infection was partially able to restore control of the infection¹⁶. To examine the antibody response in Ctrl versus KO mice, mice were infected with γ HV68 for 35 days and sera was collected. The levels of anti- γ HV68 IgG were the identical between Ctrl and KO mice, though Th1-associated IgG2c was significantly decreased in KO mice, while Th2-associated IgG1 was significantly elevated, when compared to Ctrl mice (Fig. 5A–C). These results suggest that ABCs are the primary secretors of anti- γ HV68 IgG2, though in their absence there is compensation by other B cell subsets resulting in increased anti- γ HV68 IgG1 antibodies.

We next asked if the γ HV68 reservoir was altered in mice without ABCs, as a portion of γ HV68-infected cells were ABCs. In particular, we posited that an altered viral reservoir could impact the ability of KO mice to control γ HV68 latency; previous findings indicate that various cell types infected by γ HV68 may display differential susceptibility to reactivation^{24,41}. To compare the viral reservoir in Ctrl and KO mice, we infected mice with a fluorescent strain, γ HV68.H2bYFP, and, at 8 days p.i., examined immune cell populations that comprise the γ HV68-infected population. We observed no difference in the proportion of infected cell populations, including T cells, DCs, macrophages, NK cells, and naïve and previously activated B cells (Fig. 5D). This suggests that the

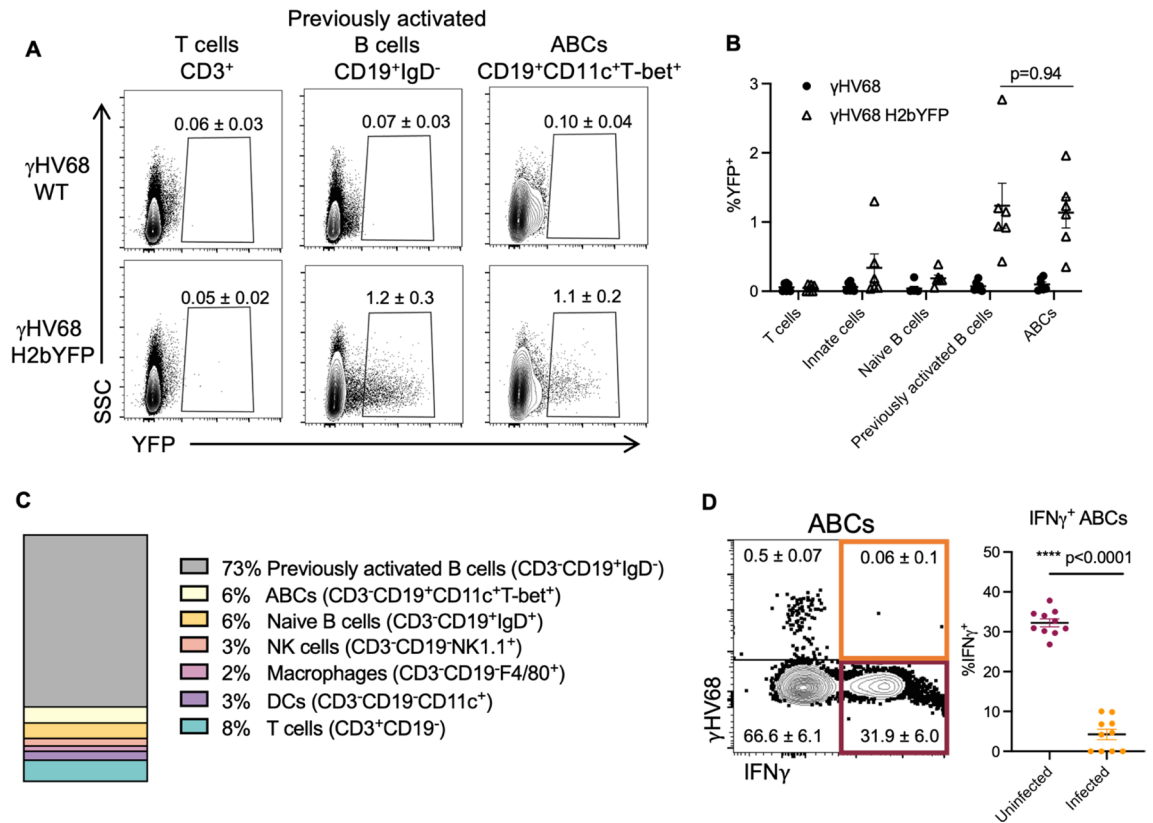


Figure 3. Analysis of ABC infection status with fluorescent γ HV68 strain. Female C57BL/6(J) mice (6 to 8-week-old at infection) infected i.p. with γ HV68 or γ HV68.H2bYFP. 8 days p.i. spleen collected and processed for flow cytometry. **(A)** Representative flow cytometry plots displaying yellow fluorescent protein (YFP) expression (x-axis) versus side-scatter (SSC, y-axis) from mice infected with γ HV68 or γ HV68.H2bYFP with mean \pm SEM. Samples gated on live, single lymphocytes, and then T cells (CD3⁺), total B cells (CD19⁺), previously activated B cells (CD19⁺IgD⁻), or ABCs (CD19⁺CD11c⁺T-bet⁺). Two samples per group concatenated for the purpose of visualization. Representative of two experiments. **(B)** Proportion of cell subsets positive for YFP expression from γ HV68-infected mice (filled circles) and γ HV68.H2bYFP-infected mice (open triangles). Each data point represents an individual mouse. **(C)** Proportion of YFP⁺ cells that are non-B cells (CD19⁻, white), non-ABC B cells (CD19⁺CD11c⁻T-bet⁻, grey), or ABCs (CD19⁺CD11c⁺T-bet⁺, black). Data n = 6 mice per group, data compiled from two experiments, representative of three experiments. **(D)** Representative flow plot of ABCs (CD19⁺CD11c⁺T-bet⁺) in the spleen gated for YFP (γ HV68.H2bYFP) and IFN γ with mean \pm SEM. Dot plot displays the proportion of either uninfected (YFP⁻) or infected (YFP⁺) ABCs in the spleen that are positive for IFN γ . **(B,D)** Data presented as mean \pm SEM, analyzed by Mann–Whitney test. Each data point represents an individual mouse. p-values indicated as asterisks as follows: ****p < 0.0001.

cell populations infected with γ HV68 are not substantially altered in KO mice compared to Ctrl mice, making it unlikely that changes to the reservoir impacted susceptibility to viral reactivation.

To ask whether ABCs influence anti-viral immune cells in the spleen, we next examined three cell populations previously shown to be important for control of latent γ HV68: IFN γ -producing cells, γ HV68-specific CD8⁺ T cells, and V β 4⁺CD8⁺ T cells. IFN γ is present at low levels during latency⁴² and is critical for controlling γ HV68 reactivation from latency^{24,25,43}. In particular, IFN γ -producing T cells are known to block γ HV68 reactivation^{24,44–46}. CD8⁺ T cells that harbor the V β 4 TCR were also examined. CD8⁺V β 4⁺ T cells expand following γ HV68 infection and reach their highest levels during latency, wherein they persist throughout infection without taking on an exhausted phenotype^{47–49}. γ HV68-specific CD8⁺ T cells were also measured with tetramers to p79, an immunodominant γ HV68 epitope for which CD8-specific memory T cells remain throughout latent infection⁵⁰. We observed that the proportion of CD4⁺ and CD8⁺ T cells that express IFN γ were unchanged between mice with and without ABCs (Fig. 5E,F). Further, no differences were observed in the proportion of either V β 4⁺CD8⁺ T cells or γ HV68 p79-specific CD8⁺ T cells between mice with and without ABC circulating populations (Fig. 5G,H). Additionally, we found that the proportion of NK cells and B cells that express IFN γ , and the MFI of IFN γ on these populations, was not changed between Ctrl and KO mice whether mock-infected or infected for 6 or 35 days (Fig. S6). That a similar proportion of B cells expressed IFN γ indicates that another B cell subset likely compensates for the loss of IFN γ -expressing ABCs. Collectively, these findings indicate that ABCs are not acting to stimulate anti-viral immune cell populations in the spleen.

Together, these data indicate that knocking out ABCs leads to dysregulation of the γ HV68 antibody response, without altering the γ HV68 reservoir or T cell populations responding to the latent virus.

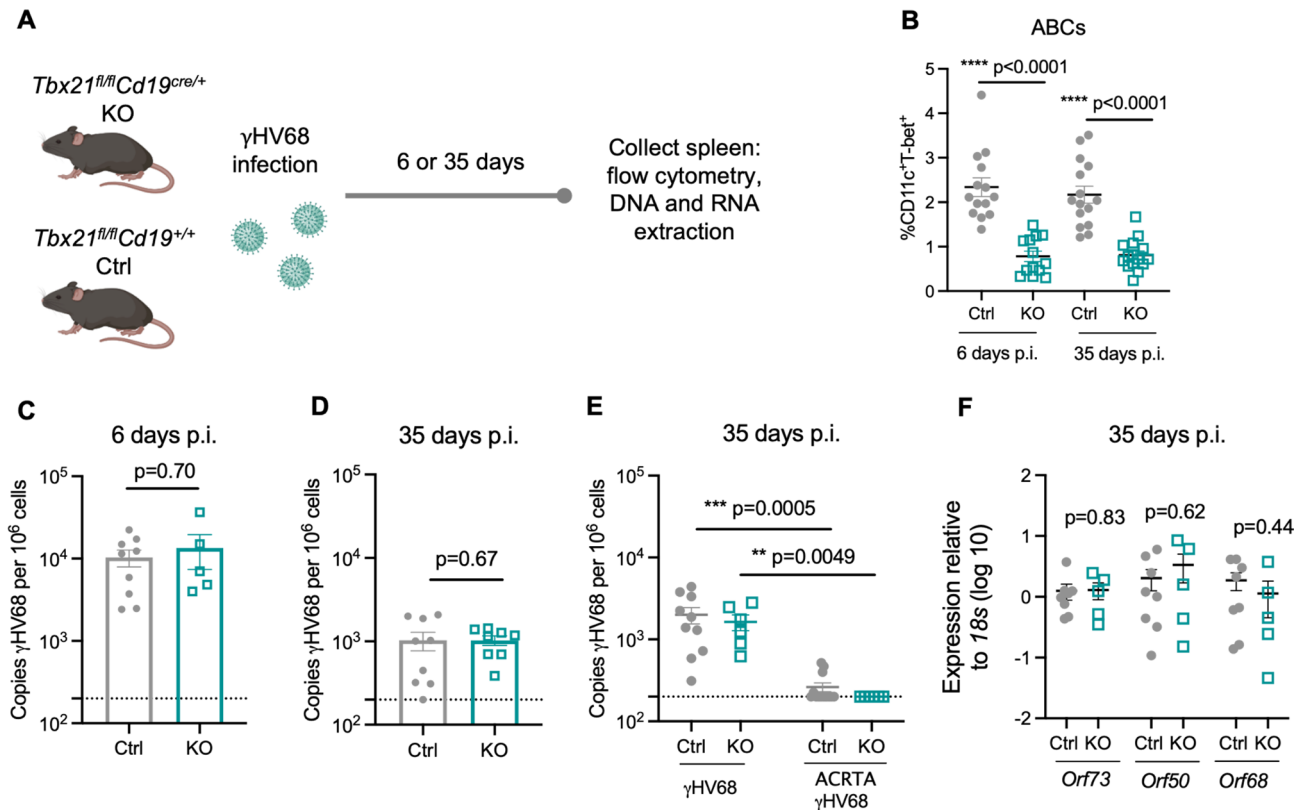


Figure 4. ABCs are not required for controlling lytic infection and achieving long-term latency. *Tbx21^{fl/fl}Cd19^{+/+}* (Ctrl, filled grey circles) and *Tbx21^{fl/fl}Cd19^{cre/+}* (KO, open blue squares) mice were infected i.p. with γHV68 or ACRTA-γHV68. 6 or 35 days p.i., spleens collected and processed for RNA extraction, DNA extraction, and flow cytometry. (A) Experimental scheme for data shown in panels (B–D,F). (B) Proportion of ABCs (CD11c⁺T-bet⁺) of previously activated B cells (CD19⁺IgD⁻) in the spleen in Ctrl and KO mice 6 and 35 days post-γHV68 infection. (C,D) Splenic γHV68 viral load (copies *Orf50* per million cells) in Ctrl (filled circles) and KO (open squares) mice as determined by qPCR day 6 and 35 p.i., with limit of detection indicated by dotted line. (E) Splenic γHV68 viral load (copies *Orf50* per million cells) in Ctrl and KO mice infected with γHV68 or ACRTA-γHV68 35 days p.i. (F) Relative expression in the spleen of *Orf73*, *Orf50*, and *Orf68* in Ctrl and KO mice at day 35 p.i. Each data point represents an individual mouse. Both male and female mice were included in the experiments. Data presented as mean ± SEM, analyzed by Mann–Whitney test (B–D,F) or Kruskal–Wallis H test (E).

In the absence of ABCs, reactivation of γHV68 occurs more readily following infections. We posited that the persistence of ABCs long-term during γHV68 and their secretion of IFN γ , TNF, and anti-viral antibodies suggest that ABCs have an important role in the suppression of latent virus reactivation. To examine this role, ex vivo reactivation assays were performed on splenocytes from Ctrl and KO mice at 35 days p.i. Splenocytes from γHV68-infected KO mice demonstrated more frequent virus reactivation in culture compared to splenocytes from γHV68-infected Ctrl mice (Fig. 6A). This finding indicates that there is an increased propensity for γHV68 reactivation in the absence of ABCs, although the assay does not disentangle whether the influence is cell-intrinsic or extrinsic nor necessarily indicate in vivo reactivation. As we did not observe elevated viral load or expression of lytic-associated genes at day 35 p.i. in KO mice (Fig. 4D,F), we speculated that although mice lacking ABCs have elevated susceptibility to reactivation, they might be able to maintain latency in steady-state conditions, though additional stressors could result in reactivation in vivo.

Therefore, to further interrogate the role of ABCs in suppressing γHV68 reactivation, we next asked if mice without ABCs are more susceptible to γHV68 reactivation following infectious challenge. Importantly, we chose to examine the response to viruses that do not typically reactivate γHV68⁵¹, such as LCMV and coxsackievirus B4 (CVB4). These heterologous viral infections were performed as physiological mimics to ask if they were sufficient to cause reactivation of latent γHV68 in the absence of ABCs. Specifically, KO and Ctrl mice were infected with γHV68 for 35 days and then challenged with LCMV or CVB4 (Fig. 6B). No clinical symptoms were observed during either of the challenges in Ctrl or KO mice and there was no difference in the relative quantity of LCMV and CVB4 in the spleens of Ctrl versus KO mice (Fig. 6C,D). Following challenge with LCMV or CVB4, mice lacking ABCs had elevated quantities of γHV68 in the spleen compared to mice with ABCs (Fig. 6E,F). We reasoned that the increased γHV68 load following challenge may be due to increased reactivation and, in support, observed increased relative expression of two lytic-associated γHV68 genes, *Orf50* and *Orf68*, in KO mice compared to Ctrl mice following challenge with the heterologous viruses (Fig. 6G,H). Alternatively, we did not

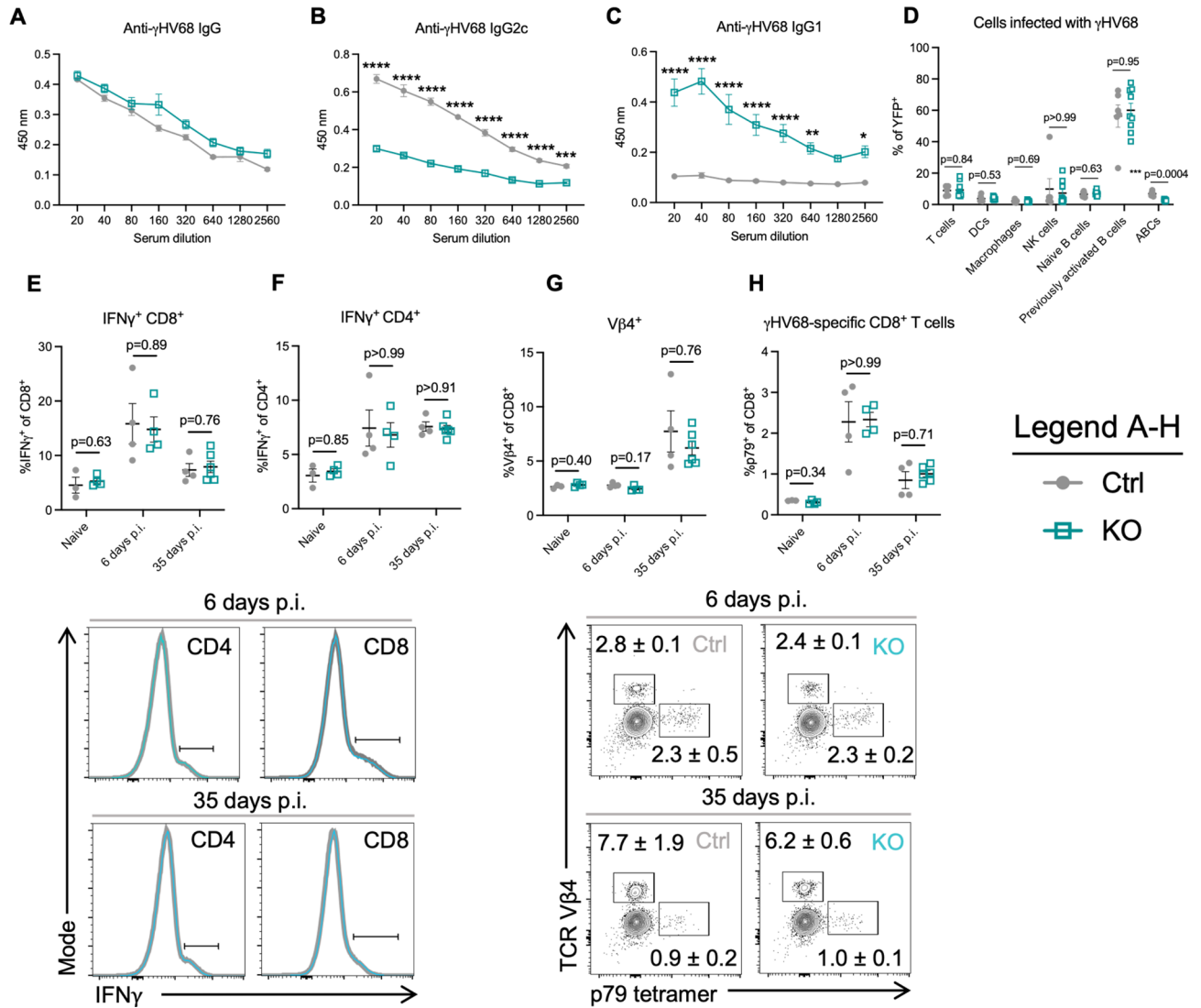


Figure 5. Mice without ABCs display a dysregulated anti- γ HV68 antibody response, though no alterations to the cell populations infected with γ HV68 or γ HV68-responding T cells, compared to mice with ABCs. (A–C) *Tbx21^{fl/fl}Cd19^{+/+}* (Ctrl, filled grey circles) and *Tbx21^{fl/fl}Cd19^{cre/+}* (KO, open blue squares) mice were infected i.p. with γ HV68 for 35 days. N=5 per group, representative of 2 experiments. (D) Ctrl and KO mice were infected i.p. with γ HV68.H2bYFP for 8 days, and various immune cell populations in the spleen analyzed for YFP expression. N=6–8 per group, data compiled from 2 experiments. (E–H) Ctrl and KO mice were infected i.p. with γ HV68 for 6 or 35 days, at which point spleens were collected for flow cytometry. Representative of 2 experiments. Flow cytometry plots are representative samples previously gated on live (E,F) CD45⁺CD3⁺ or (G,H) CD45⁺CD3⁺CD8⁺ splenocytes, with mean \pm SEM. Each data point represents an individual mouse. Both male and female mice included in experiments. Data presented as mean \pm SEM. Analyzed by two-way ANOVA (A–C) or Mann–Whitney test (D–H). p-values indicated as asterisks as follows: ****p < 0.0001, ***p < 0.001, **p < 0.01, *p < 0.05.

observe a difference in expression of the latency-associated gene *Orf73*, between Ctrl and KO mice (Fig. 6I). This also indicates that it is not simply an expansion in the number of latently infected B cells in the spleen and is a change in the active lytic expression of more virus. Further, we did not observe significant cell number increases in B cells between the KO and Ctrl mice post challenge (Fig. S7). These findings make clear that ABCs act to impede latent γ HV68 reactivation in the face of mild stresses such as heterologous infection.

Discussion

Here we have shown that ABCs are increased during acute γ HV68 infection and persist during latency for at least 150 days. Previous studies have shown that ABCs persist following clearance of viral infections¹⁰ and during chronic infection¹⁶, though their contribution during a latent infection was unexplored. Our results demonstrate a novel role for ABCs: they continuously respond in an effector manner to latent viral infection by secreting

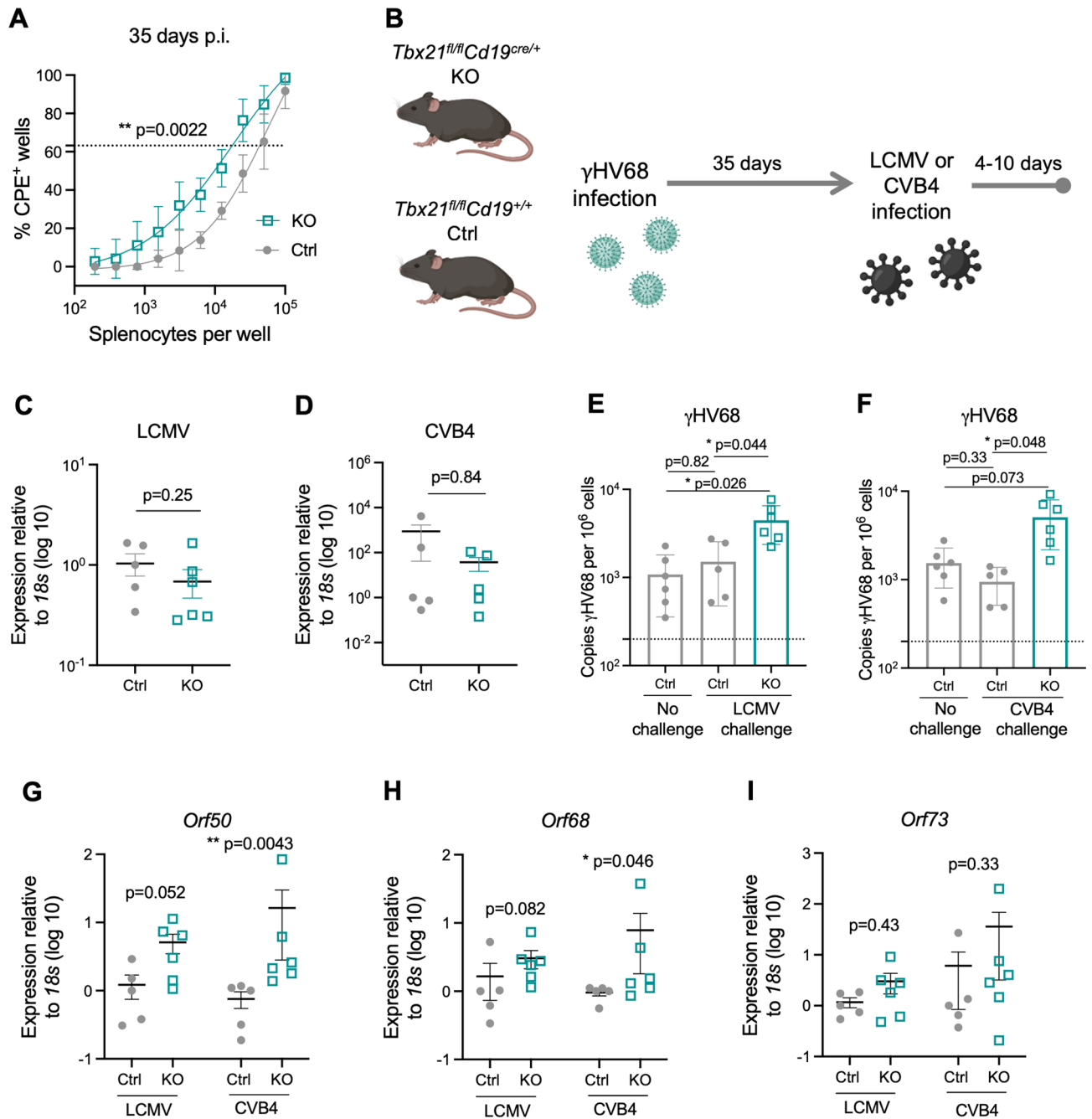


Figure 6. ABC knockout mice are more susceptible to reactivation. (A) *Tbx21^{fl/fl}Cd19^{cre/+}* (Ctrl, filled grey circles) and *Tbx21^{fl/fl}Cd19^{+/+}* (KO, open blue squares) mice were infected i.p. with γ HV68. 35 days p.i., spleens were collected and processed for reactivation assay. N = 6 mice per group, data compiled from two independent experiments. (B) Experimental scheme for data shown in panels (C–I). Ctrl and KO mice were infected i.p. with γ HV68 for 35 days and then challenged with either LCMV (Armstrong) or CVB4 for 10 to 4 days, respectively. (C–I) Spleens collected, processed, and DNA and RNA was extracted from total splenocytes following RBC lysis. (C,D) Relative expression of LCMV (C) and CVB4 (D) between Ctrl and KO mice measured by RT-qPCR. (E,F) Copies of γ HV68 detected by qPCR in the spleen per million cells following challenge with LCMV or CVB4. (G–I) Relative expression in the spleen of *Orf73*, *Orf50*, and *Orf68* in Ctrl and KO mice. Each data point represents an individual mouse. Both male and female mice included in experiments. Data presented as mean \pm SEM, analyzed by Mann–Whitney test (A,C,D,G–I) or one-way ANOVA (E,F). p-values indicated as asterix as follows: **p < 0.01, *p < 0.05.

anti-viral cytokines and antibodies. Further, our results indicate that ABCs may play an important role in suppressing γ HV68 reactivation during subsequent heterologous infectious challenges.

Our results show that ABCs continuously express anti-viral cytokines during latency and the presence of the latent virus is required for the sustained anti-viral cytokine expression by ABCs. Compared to other B cells, ABCs display uniquely high expression of anti-viral cytokines IFN γ and TNF during γ HV68. In addition to expressing cytokines, ABCs also produce anti-viral antibodies, as deficiency of ABCs results in a significant loss of γ HV68-specific IgG2c antibodies. We hypothesized that the production of anti-viral cytokines and antibodies by ABCs could be a way in which ABCs restrain γ HV68 reactivation. Using mice deficient in ABCs, we showed that ABCs are important for the suppression of γ HV68 reactivation in the face of heterologous viral challenge.

A surprising finding of our study is that ABCs are increased more so in female than male mice throughout γ HV68 infection, in both the blood and spleen. Sex-differences are well-documented in anti-viral immune responses⁵² and ABCs have previously been shown to display a female sex bias in contexts of aging and autoimmunity^{4,53}. It has recently been shown that the ABC female sex bias in lupus mice is abolished following the duplication of *Tlr7* in male mice⁵³. While we show that there is no difference in the quantity of γ HV68 between female and male mice, TLR7 stimulation is known to be important for ABC differentiation^{3,4} and TLR7 is critical for the control of lytic γ HV68 infection and maintenance of latency⁵⁴. While increased frequencies of ABCs were observed in female mice compared to males, we found that a similar proportion of the ABCs express anti-viral cytokines in both males and females. No differences between male and female mice were observed in viral load or reactivation.

Using a parallel approach to knockout T-bet in B cells with bone marrow chimeras, it was previously shown that mice lacking ABCs display an increased quantity of γ HV68 during the early stage of latency, at day 18 p.i., compared to controls⁷. This difference with our results is most easily explained by the fact that the two studies measure viral titre at different timepoints (day 18 p.i., the early-stage latency versus day 35 p.i., long-term latency). These two timepoints are distinct, with viral reactivation occurring more frequently at early-stage compared to long-term latency²⁸. Additionally, it is well known that γ HV68 latency establishment can be delayed by certain immunological perturbations, such as loss of transcription factor NF- κ B⁵⁵. Therefore, we propose the possibility that mice without ABCs display a delayed establishment of latency and/or elevated viral reactivation during early latency under steady-state conditions, resulting in elevated viral titers at an early latency timepoint, though no difference during long-term latency. Our results also highlight elevated viral reactivation *ex vivo* during long-term latency and demonstrate a loss of latency maintenance in the face of heterologous challenge. The results of these two studies together indicate that mice lacking ABCs display elevated viral reactivation and hint at potential differences in the kinetics of latency establishment in the absence of ABCs. Additionally, these two studies differ in the inoculating dose (lower herein) and the method of ABC knockout, which could also contribute to the observed differences.

ABCs are known to possess an array of functional capacities and the precise mechanism(s) of ABC contribution to the restraint of γ HV68 reactivation will be the focus of future studies. Here we have shown that only the antibody response is altered in mice deficient in ABCs and unexpectedly, changes are not observed in the anti-viral T cell response or viral reservoir. The ability of ABCs to continuously secrete anti-viral cytokines during latent infection is an additional mechanism that likely contributes to the suppression of γ HV68 reactivation. Understanding the precise localization of ABCs in relation to γ HV68-infected B cells will also aid in our understanding of the development of splenic structures, in particular germinal centres, as ABCs have been shown to play a role in their development⁵⁶. In future it will also be worthwhile to perform intranasal inoculations, in comparison to the intraperitoneal route that was used here, to investigate a potential role of ABCs at mucosal barriers.

Whether ABCs play a role in suppressing the reactivation of human gamma-herpesvirus infections such as Epstein-Barr virus (EBV) and Kaposi sarcoma-associated herpesvirus, is not known. Understanding this role would have important relevance in diseases associated with these human gammaherpesviruses, including various malignancies, myalgic encephalomyelitis/chronic fatigue syndrome, and chronic-active EBV⁵⁷⁻⁵⁹.

This work demonstrates that ABCs are a long-lasting effector population during γ HV68 latent infection. ABCs are likely one of many players in the maintenance of latent infection and have a unique role in the control of latent virus reactivation following subsequent heterologous infections.

Methods

Mice. *Tbx21^{fl/fl}Cd19^{cre/+}* mice were generated by crossing *Tbx21^{fl/fl}Cd19^{cre/+}* and *Tbx21^{fl/fl}Cd19^{+/+}* mice with *Tbx21^{fl/fl}* and *Cd19^{cre/+}* mice provided by Dr. Pippa Marrack⁵⁶. C57BL/6(J) mice were originally purchased from The Jackson Laboratory and all animals were bred and maintained under specific-pathogen free conditions in the animal facility at the University of British Columbia. Mice were housed in individually ventilated cages in groups of up to five animals with unrestricted access to food and water. All animal work was approved by the Canadian Council for Animal Care (Protocols A17-0105, A17-0184) and performed in accordance with relevant guidelines and regulations, following recommendations in the ARRIVE guidelines.

γ HV68, ACRTA- γ HV68, and γ HV68H2B.YFP infection. γ HV68 WUMS strain (ATCC), ACRTA- γ HV68 (developed by Dr. Ting-Ting Wu, gift of Dr. Marcia A. Blackman)³¹, and γ HV68H2B.YFP (developed and provided by Dr. Samuel H. Speck) were propagated in Baby Hamster Kidney cells (BHK, ATCC). Viruses were diluted in Minimum Essential Media (MEM) prior to infection and maintained on ice. 6- to 8-week-old mice were infected i.p. with 10⁴ PFU of γ HV68, ACRTA- γ HV68, γ HV68H2B.YFP, or mock-infected with MEM as previously described. Clinical symptoms were not observed during γ HV68, ACRTA- γ HV68, or γ HV68H2B.YFP infections in C57BL/6(J) nor *Tbx21^{fl/fl}Cd19^{cre/+}* or *Tbx21^{fl/fl}Cd19^{+/+}* mice.

Antigen	Fluor	Clone	Dilution	Company
CD3e	eFluor 450	500A2	1:200	Thermo Fisher Scientific
CD19	PE	1D3	1:200	Thermo Fisher Scientific
CD19	Pe-Cy7	1D3	1:200	Thermo Fisher Scientific
CD19	SB780	1D3	1:100	Thermo Fisher Scientific
IgD	Pe-Cy7	11-26	1:200	Thermo Fisher Scientific
CD11c	Alexafluor700	N418	1:100	Thermo Fisher Scientific
CD11c	APC	N418	1:100	Biologend
T-bet	PerCpCy5.5	4B10	1:100	Thermo Fisher Scientific
IFN γ	APC	XMG1.2	1:100	Thermo Fisher Scientific
TNF	Pe-Cy7	MP6-XT22	1:100	Biologend
IL-17A	PEDazzle594	TC11-18H10.1	1:100	Biologend
CD45	Alexafluor700	30-F11	1:200	Thermo Fisher Scientific
CD45	APC-eFluor 780	30-F11	1:200	Thermo Fisher Scientific
CD4	SB645	RM4-5	1:100	Thermo Fisher Scientific
CD8	APC-eFluor 780	53-6.7	1:200	Thermo Fisher Scientific
CD8	PEDazzle594	53-6.7	1:100	Biologend
CD11b	Pe-Cy7	M1/70	1:100	Thermo Fisher Scientific
Ly6G	PerCpCy5.5	RB6-8C5	1:100	Thermo Fisher Scientific
CD335	FitC	29A1.4	1:100	Thermo Fisher Scientific
NK1.1	PE	PK136	1:100	Thermo Fisher Scientific
F4/80	APC-eFluor 780	BM8	1:100	Thermo Fisher Scientific
CD62L	PerCpCy5.5	MEL-14	1:100	Thermo Fisher Scientific
CD44	Alexafluor700	IM7	1:200	Thermo Fisher Scientific
PD1	PerCpCy5.5	RMP1-30	1:100	Thermo Fisher Scientific
CXCR5	PE	SPRCL5	1:100	Thermo Fisher Scientific
FoxP3	Alexafluor700	FJK-16s	1:100	Thermo Fisher Scientific
CD138	PEDazzle594	281-2	1:100	Biologend
CD95	FitC	SA367H8	1:100	Biologend
IgM	APCCy7	RMM-1	1:100	Biologend
TCR V β 4	FitC	KT4	1:100	BD Bioscience

Table 1. Flow cytometry antibodies.

LCMV infection. LCMV Armstrong strain 53b (originally acquired from Dr. M.B. Oldstone) was propagated on BHK cells. Prior to infection, virus was diluted in RPMI-1640 media (Gibco) and maintained on ice. Mice (11- to 13-week-old) were infected i.p. with 2×10^5 PFU LCMV or mock infected with media. No clinical symptoms were observed from LCMV infection in *Tbx21^{fl/fl}Cd19^{cre/+}* nor *Tbx21^{fl/fl}Cd19^{+/+}* mice.

CVB4 infection. CVB4 Edward strain was propagated on HeLa cells and titred by plaque assay. Virus was diluted in Dulbecco's Modified Eagle Medium (DMEM, Gibco) and maintained on ice prior to infection. Mice (11- to 13-week-old) were infected i.p. with 100 PFU CBV4. No clinical symptoms were observed from CVB4 infection in *Tbx21^{fl/fl}Cd19^{cre/+}* or *Tbx21^{fl/fl}Cd19^{+/+}* mice.

Tissue harvesting and processing for flow cytometry. Mice were anaesthetised with isoflurane and euthanized by cardiac puncture. For flow cytometry, blood was collected by cardiac puncture into 100 μ l 0.5 M Ethylenediaminetetraacetic acid (EDTA) to prevent clotting and placed on ice until processing. Spleen extracted and placed into 2 ml PBS and kept on ice until processing. Blood was incubated in 10 ml warmed (37 °C) ACK lysis buffer for 15 min at room temperature to remove red blood cells and washed twice with FACS buffer. Splens were mashed through a 70 μ m cell strainer with a 3 ml syringe insert to make a single cell suspension for each sample. Splenocytes were incubated in 4 ml warmed (37 °C) ACK lysis buffer for 10 min on ice to lyse red blood cells and remaining cells were resuspended in FACS buffer and kept on ice until further use.

Flow cytometry analysis of cell-type specific surface antigens and intracellular cytokines. For analysis of extracellular and intracellular antigens, 2 million cells per spleen sample or all cells collected per blood sample were stained with appropriate antibodies. Prior to staining, samples were incubated at 4 °C covered from light for 30 min with 2 μ l/ml Fixable Viability Dye eFluor506 (Thermo Fisher) while in PBS and then resuspended in rat anti-mouse CD16/32 (Fc block, BD Biosciences) antibody for 10 min. Then, samples were stained with fluorochrome labeled antibodies (Table 1) against cell surface antigens for 30 min covered from light at 4 °C, washed, and resuspended in Fix/Perm buffer (Thermo Fisher) for 30 min-12 h while maintained covered from light at 4 °C. Samples were then washed twice with perm buffer and incubated 40 min with anti-

Gene	Sequence
<i>Ptger2</i> Forward Primer	5'-TACCTTCAGCTGTACGCCAC-3'
<i>Ptger2</i> Reverse Primer	5'-GCCAGGAGAATGAGGTGGTC-3'
<i>Ptger2</i> Probe	5'-/56-FAM/CCTGCTGCT/ZEN/TATCGTGGCTG/3IABkFQ/-3'
<i>Orf50</i> Forward Primer	5'-TGGACTTTGACAGCCCAGTA-3'
<i>Orf50</i> Reverse Primer	5'-TCCCTTGAGGCAAATGATTC-3'
<i>Orf50</i> Probe	5'-/56-FAM/TGACAGTGC/ZEN/CTATGGCCAAGTCTTG/3IABkFQ/-3'

Table 2. γ HV68 qPCR primers and probe sequences.

Gene	Sequence
<i>Orf50</i> forward	5'-GGCCGCAGACATTTAATGAC-3'
<i>Orf50</i> reverse	5'-GCCTCAACTTCTCTGGATATGCC-3'
<i>Orf73</i> forward	5'-AAGGGTTGTCTTGGCCTAC TGTG-3'
<i>Orf73</i> reverse	5'-AGAGATGCTGTGGGACCATGTTG-3'
<i>Orf68</i> forward	5'-CTCAAATACACTGGCCGCCATC-3'
<i>Orf68</i> reverse	5'-CGTGCTTGAGATATGAGTGAGT-3'
<i>CVB4</i> forward	5'-CCCACAGGACGCTCTAATA-3'
<i>CVB4</i> reverse	5'-CAGAGTTACCCGTTACGACA-3'
<i>LCMV GP</i> forward	5'-TGCTGACCAAATGGATGATT-3'
<i>LCMV GP</i> reverse	5'-CTGCTGTGTTCCCGAAACACT-3'
<i>18s</i> forward	5'-GTAACCCGTTGAACCCATT-3'
<i>18s</i> reverse	5'-CCATCCAATCGGTAGTAGCG-3'

Table 3. qPCR for lytic and latent γ HV68 genes primer sequences.

bodies for intracellular antigens (Table 1) in Perm buffer at covered from light at RT. Cells were then washed and resuspended in FACS buffer with 2 mM EDTA. For analysis of cytokine production, 4 million cells per sample were stimulated ex vivo for 3 h at 5% CO₂ at 37 °C in Minimum Essential Media (Gibco) containing 10% fetal bovine serum (FBS, Sigma-Aldrich), 1 μ l/ml GolgiPlug (BD Biosciences), 10 ng/ml PMA (Sigma-Aldrich) and 500 ng/ml ionomycin (Thermo Fisher) and washed prior to staining. Samples were collected on an Attune NxT Flow Cytometer (Thermo Fisher) and analyzed with FlowJo software v10 (FlowJo LLC).

Tetramer staining. γ HV68-specific CD8 T cells were identified by staining with a tetramer acquired from the NIH Tetramer Facility. 2 million cells per well were incubated for 1 h at RT with p79 (K^b /ORF61₅₂₄₋₅₃₁ TSIN-FVKI, diluted 1:400) following viability staining and Fc receptor block, as described above, but before extracellular antigen staining. Uninfected mice stained with tetramers used as negative gating controls.

γ HV68 qPCR. DNA was isolated from 4×10^6 splenocytes using PureLink™ Genomic DNA Mini Kit (Thermo Fisher) and quantified with a spectrophotometer. qPCR was performed using $2 \times$ QuantiNova Probe Mastermix (Qiagen, USA) on the Bio-Rad CFX96 Touch™ Real Time PCR Detection system. Copies of γ HV68 were quantified in duplicate wells with 150 ng DNA per reaction using primers and probes specific to γ HV68 *Orf50* and mouse *Ptger2* (Table 2). Standard curves were obtained by serial dilutions of *Orf50* and *Ptger2* gBlocks (*Orf50*: 2×10^6 – 2×10^1 ; *Ptger2*: 5×10^7 – 5×10^2) that were amplified in parallel.

RT-qPCR for γ HV68 lytic and latency-associated genes and relative quantity of LCMV and CVB4. Portion of spleen stabilized in RNAlater immediately following collection and stored at -80 °C for up to 12 weeks. RNA extracted with RNeasy mini kit (Qiagen, cat no. 74104) and cDNA immediately synthesized with High-Capacity cDNA Reverse Transcription Kit (Thermo Fisher, cat no. 4368814). Reaction performed with 500 ng per reaction in duplicate wells and cDNA quantified with a spectrophotometer. qPCR was performed using iQTM SYBR® Green supermix (Bio-Rad) on the Bio-Rad CFX96 Touch™ Real Time PCR Detection system. Transcript specific primers have been previously described for *Orf50*, *Orf73*, and *Orf68*⁶⁰, LCMV⁶¹, and CVB4⁶² and ordered from Integrated DNA Technologies (Table 3). *Orf50*, *Orf73*, and *Orf68* expression normalized to the ribosomal housekeeping gene *18s* using the $2^{-\Delta\Delta Ct}$ method with expression determined relative to median value in Ctrl group.

Ex vivo limiting dilution reactivation assay. A single cell suspension following RBC lysis with ACK lysis buffer was prepared from freshly collected spleens. To analyze ex vivo reactivation, limiting dilution reactivation assay was performed as previously described¹⁸. Twofold serial dilutions of splenocytes starting at 10^5 cells

per well were plated onto monolayer of mouse embryonic fibroblast (MEF, C57BL/6) cells (ATCC) in 96-well flat-bottom polystyrene tissue culture plates. Twelve wells were plated per dilution. Plates were incubated at 37 °C 5% CO₂ for 10 days and scored for microscopically for viral cytopathic effects (CPE). Data were plotted as sigmoidal dose curves and interpolation was used to determine the cell density per sample at which 63.2% of wells were positive for CPE.

Anti-γHV68 antibodies. Serum was collected via cardiac puncture and maintained at RT to allow for clotting. The sera were isolated by centrifugation 2000×g for 10 min, aliquoted, and stored for up to 12 months at −80 °C prior to running the ELISA. Anti-γHV68 antibodies were quantified by standard indirect ELISA. Briefly, γHV68 virions were inactivated in 4% paraformaldehyde (PFA) for 20 min at RT. Then, ELISA plates (NUNC, Thermo Fisher) were coated with 5 μg/ml γHV68 in coating buffer (0.05 M NaHCO₃, pH 9.6) with 1% PFA overnight at 4 °C. The plate was then washed 4× with wash buffer (PBS-0.05% Tween-20), blocked in blocking buffer (5% NBCS in PBS) for 1 h at 37 °C, and incubated with serial dilutions (1:20, 1:40, 1:80, 1:160, 1:320, 1:640, 1:1280, 1:2560) of test sera diluted in blocking buffer for 2 h at 37 °C. The plate was washed 4× with wash buffer and bound antibody was incubated with HRP-conjugated goat anti-mouse IgG (Thermo Fisher), rat anti-mouse IgG1 (BD Biosciences), or goat anti-mouse IgG2c (Thermo Fisher), all diluted 1:500 in blocking buffer, for 1 h at 37 °C, washed 4× with wash buffer, and detected by TMB substrate (BD Biosciences). Absorbance was read at 450 nm on a VarioSkan Plate Reader (Thermo Fisher).

Statistical analyses. Data analysis and presentation as well as statistical tests were performed using GraphPad Prism software 8.4.2 (GraphPad Software Inc.). Results are presented as mean ± SEM. Statistical tests, significance (p-value), sample size (n, number of mice per group) and number of experimental replicates are stated in the figure legends. Statistical analyses included: two-way ANOVA with Geisser-Greenhouse's correction, Mann-Whitney test, and one-way ANOVA. P-values indicated by asterisks as follows: ****p < 0.0001, ***p < 0.001, **p < 0.01, *p < 0.05.

Study approval. All work was approved by the Animal Care Committee (ACC) of the University of British Columbia (Protocols A17-0105, A17-0184).

Data availability

All data generated or analysed during this study are included in this published article and its Supplementary Information files.

Received: 6 July 2022; Accepted: 30 November 2022

Published online: 07 December 2022

References

- Dong, S., Forrest, J. C. & Liang, X. Murine gammaherpesvirus 68: A small animal model for gammaherpesvirus-associated diseases. In *Infectious Agents Associated Cancers: Epidemiology and Molecular Biology* (eds Cai, Q. *et al.*) 225–236 (Springer, 2017).
- Barton, E., Mandal, P. & Speck, S. H. Pathogenesis and host control of gammaherpesviruses: Lessons from the mouse. *Annu. Rev. Immunol.* **29**, 351–397. <https://doi.org/10.1146/annurev-immunol-072710-081639> (2011).
- Hao, Y., O'Neill, P., Naradikian, M. S., Scholz, J. L. & Cancro, M. P. A B-cell subset uniquely responsive to innate stimuli accumulates in aged mice. *Blood* **118**(5), 1294–1304. <https://doi.org/10.1182/blood-2011-01-330530> (2011).
- Rubtsov, A. V. *et al.* Toll-like receptor 7 (TLR7)-driven accumulation of a novel CD11c+ B-cell population is important for the development of autoimmunity. *Blood* **118**(5), 1305–1315. <https://doi.org/10.1182/blood-2011-01-331462> (2011).
- Cancro, M. P. Age-associated B cells. *Cells Annu. Rev. Immunol.* **38**(1), 315–340. <https://doi.org/10.1146/annurev-immunol-092419-031130> (2020).
- Mouat, I. C. & Horwitz, M. S. Age-associated B cells in viral infection. *PLoS Pathog.* **18**(3), e1010297. <https://doi.org/10.1371/journal.ppat.1010297> (2022).
- Rubtsova, K., Rubtsov, A. V., van Dyk, L. F., Kappler, J. W. & Marrack, P. T-box transcription factor T-bet, a key player in a unique type of B-cell activation essential for effective viral clearance. *Proc. Natl. Acad. Sci.* **110**(34), E3216–E3224. <https://doi.org/10.1073/pnas.1312348110> (2013).
- Rubtsova, K. *et al.* T Cell production of IFNγ in response to TLR7/IL-12 stimulates optimal B cell responses to viruses. *PLoS ONE* **11**(11), e0166322. <https://doi.org/10.1371/journal.pone.0166322> (2016).
- Knox, J. J. *et al.* T-bet+ B cells are induced by human viral infections and dominate the HIV gp140 response. *JCI Insight* **2**(8), 92943. <https://doi.org/10.1172/jci.insight.92943> (2017).
- Johnson, J. L. *et al.* The transcription factor T-bet resolves memory B cell subsets with distinct tissue distributions and antibody specificities in mice and humans. *Immunity*. <https://doi.org/10.1016/j.immuni.2020.03.020> (2020).
- Eccles, J. D. *et al.* T-bet+ memory B cells link to local cross-reactive IgG upon human rhinovirus infection. *Cell Rep.* **30**(2), 351–366. <https://doi.org/10.1016/j.celrep.2019.12.027> (2020).
- Woodruff, M. C. *et al.* Extrafollicular B cell responses correlate with neutralizing antibodies and morbidity in COVID-19. *Nat. Immunol.* **21**(12), 1506–1516. <https://doi.org/10.1038/s41590-020-00814-z> (2020).
- Rubtsov, A. V. *et al.* CD11c-expressing B cells are located at the T cell/B cell border in spleen and are potent APCs. *J. Immunol. Baltim. Md.* **195**(1), 71–79. <https://doi.org/10.4049/jimmunol.1500055> (2015).
- Mendoza, A. *et al.* Assembly of a spatial circuit of T-bet-expressing T and B lymphocytes is required for antiviral humoral immunity. *Sci. Immunol.* **6**(60), 4710. <https://doi.org/10.1126/sciimmunol.abi4710> (2021).
- Peng, S. L., Szabo, S. J. & Glimcher, L. H. T-bet regulates IgG class switching and pathogenic autoantibody production. *Proc. Natl. Acad. Sci. U.S.A.* **99**(8), 5545–5550. <https://doi.org/10.1073/pnas.082114899> (2002).
- Barnett, B. E. *et al.* B cell intrinsic T-bet expression is required to control chronic viral infection. *J. Immunol. Baltim. Md.* **197**(4), 1017–1022. <https://doi.org/10.4049/jimmunol.1500368> (2016).
- Ehtisham, S., Sunil-Chandra, N. P. & Nash, A. A. Pathogenesis of murine gammaherpesvirus infection in mice deficient in CD4 and CD8 T cells. *J. Virol.* **67**(9), 5247–5252. <https://doi.org/10.1128/JVI.67.9.5247-5252.1993> (1993).

18. Weck, K. E., Barkon, M. L., Yoo, L. I., Speck, S. H. & Virgin, H. W. IV. Mature B cells are required for acute splenic infection, but not for establishment of latency, by murine gammaherpesvirus 68. *J. Virol.* **70**(10), 6775–6780. <https://doi.org/10.1128/JVI.70.10.6775-6780.1996> (1996).
19. Willer, D. O. & Speck, S. H. Long-term latent murine gammaherpesvirus 68 infection is preferentially found within the surface immunoglobulin D-negative subset of splenic B cells in vivo. *J. Virol.* **77**(15), 8310–8321. <https://doi.org/10.1128/JVI.77.15.8310-8321.2003> (2003).
20. Simas, J. P., Swann, D., Bowden, R. & Efstathiou, S. Analysis of murine gammaherpesvirus-68 transcription during lytic and latent infection. *J. Gen. Virol.* **80**(Pt 1), 75–82. <https://doi.org/10.1099/0022-1317-80-1-75> (1999).
21. Kim, I. J., Flaño, E., Woodland, D. L. & Blackman, M. A. Antibody-mediated control of persistent gamma-herpesvirus infection. *J. Immunol. Baltim. Md.* **168**(8), 3958–3964. <https://doi.org/10.4049/jimmunol.168.8.3958> (2002).
22. Freeman, M. L. *et al.* Importance of antibody in virus infection and vaccine-mediated protection by a latency-deficient recombinant murine γ -herpesvirus-68. *J. Immunol. Baltim. Md.* **188**(3), 1049–1056. <https://doi.org/10.4049/jimmunol.1102621> (2012).
23. Stevenson, P. G., Cardin, R. D., Christensen, J. P. & Doherty, P. C. Immunological control of a murine gammaherpesvirus independent of CD8+ T cells. *J. Gen. Virol.* **80**(Pt 2), 477–483. <https://doi.org/10.1099/0022-1317-80-2-477> (1999).
24. Steed, A., Buch, T., Waisman, A. & Virgin, H. W. Gamma interferon blocks gammaherpesvirus reactivation from latency in a cell type-specific manner. *J. Virol.* **81**(11), 6134–6140. <https://doi.org/10.1128/JVI.00108-07> (2007).
25. Goodwin, M. M., Canny, S., Steed, A. & Virgin, H. W. Murine gammaherpesvirus 68 has evolved gamma interferon and stat1-repressible promoters for the lytic switch gene 50. *J. Virol.* **84**(7), 3711–3717. <https://doi.org/10.1128/JVI.02099-09> (2010).
26. Stewart, J. P., Usherwood, E. J., Ross, A., Dyson, H. & Nash, T. Lung epithelial cells are a major site of murine gammaherpesvirus persistence. *J. Exp. Med.* **187**(12), 1941–1951 (1998).
27. Usherwood, E. J., Stewart, J. P., Robertson, K., Allen, D. J. & Nash, A. A. Absence of splenic latency in murine gammaherpesvirus 68-infected B cell-deficient mice. *J. Gen. Virol.* **77**(Pt 11), 2819–2825. <https://doi.org/10.1099/0022-1317-77-11-2819> (1996).
28. Weck, K. E., Kim, S. S., Virgin, H. W. & Speck, S. H. B cells regulate murine gammaherpesvirus 68 latency. *J. Virol.* **73**(6), 4651–4661 (1999).
29. Siegel, A. M., Rangaswamy, U. S., Napier, R. J. & Speck, S. H. Blimp-1-dependent plasma cell differentiation is required for efficient maintenance of murine gammaherpesvirus latency and antiviral antibody responses. *J. Virol.* **84**(2), 674–685. <https://doi.org/10.1128/JVI.01306-09> (2010).
30. Mouat, I. C. *et al.* Gammaherpesvirus infection drives age-associated B cells toward pathogenicity in EAE and MS. *Sci. Adv.* **8**(47), <https://doi.org/10.1126/sciadv.ade6844> (2022).
31. Jia, Q. *et al.* Induction of protective immunity against murine gammaherpesvirus 68 infection in the absence of viral latency. *J. Virol.* **84**(5), 2453–2465. <https://doi.org/10.1128/JVI.01543-09> (2010).
32. Flaño, E., Husain, S. M., Sample, J. T., Woodland, D. L. & Blackman, M. A. Latent murine gamma-herpesvirus infection is established in activated B cells, dendritic cells, and macrophages. *J. Immunol. Baltim. Md.* **165**(2), 1074–1081. <https://doi.org/10.4049/jimmunol.165.2.1074> (2000).
33. Sunil-Chandra, N. P., Efstathiou, S. & Nash, A. A. Murine gammaherpesvirus 68 establishes a latent infection in mouse B lymphocytes in vivo. *J. Gen. Virol.* **73**(Pt 12), 3275–3279. <https://doi.org/10.1099/0022-1317-73-12-3275> (1992).
34. Marques, S., Efstathiou, S., Smith, K. G., Haury, M. & Simas, J. P. Selective gene expression of latent murine gammaherpesvirus 68 in B lymphocytes. *J. Virol.* **77**(13), 7308–7318. <https://doi.org/10.1128/JVI.77.13.7308-7318.2003> (2003).
35. Collins, C. M., Boss, J. M. & Speck, S. H. Identification of infected B-cell populations by using a recombinant murine gammaherpesvirus 68 expressing a fluorescent protein. *J. Virol.* **83**(13), 6484–6493. <https://doi.org/10.1128/JVI.00297-09> (2009).
36. Collins, C. M. & Speck, S. H. Tracking murine gammaherpesvirus 68 infection of germinal center B cells in vivo. *PLoS ONE* **7**(3), e33230. <https://doi.org/10.1371/journal.pone.0033230> (2012).
37. Staudt, M. R. & Dittmer, D. P. The Rta/Orf50 transactivator proteins of the gamma-herpesviridae. *Curr. Top. Microbiol. Immunol.* **312**, 71–100. https://doi.org/10.1007/978-3-540-34344-8_3 (2007).
38. Didychuk, A. L. *et al.* A pentameric protein ring with novel architecture is required for herpesviral packaging. *eLife* **10**, e62261. <https://doi.org/10.7554/eLife.62261> (2021).
39. Fowler, P., Marques, S., Simas, J. P. & Efstathiou, S. ORF73 of murine herpesvirus-68 is critical for the establishment and maintenance of latency. *J. Gen. Virol.* **84**(Pt 12), 3405–3416. <https://doi.org/10.1099/vir.0.19594-0> (2003).
40. Moorman, N. J., Willer, D. O. & Speck, S. H. The gammaherpesvirus 68 latency-associated nuclear antigen homolog is critical for the establishment of splenic latency. *J. Virol.* **77**(19), 10295–10303. <https://doi.org/10.1128/jvi.77.19.10295-10303.2003> (2003).
41. Wang, G. *et al.* Th2 cytokine modulates herpesvirus reactivation in a cell type specific manner. *J. Virol.* <https://doi.org/10.1128/JVI.01946-20> (2021).
42. Barton, E. S. *et al.* Herpesvirus latency confers symbiotic protection from bacterial infection. *Nature* **447**(7142), 326–329. <https://doi.org/10.1038/nature05762> (2007).
43. Tibbetts, S. A., van Dyk, L. F., Speck, S. H. & Virgin, H. W. Immune control of the number and reactivation phenotype of cells latently infected with a gammaherpesvirus. *J. Virol.* **76**(14), 7125–7132. <https://doi.org/10.1128/JVI.76.14.7125-7132.2002> (2002).
44. Gredmark-Russ, S., Cheung, E. J., Isaacson, M. K., Ploegh, H. L. & Grotenbreg, G. M. The CD8 T-cell response against murine gammaherpesvirus 68 is directed toward a broad repertoire of epitopes from both early and late antigens. *J. Virol.* **82**(24), 12205–12212. <https://doi.org/10.1128/JVI.01463-08> (2008).
45. Steed, A. L. *et al.* Gamma interferon blocks gammaherpesvirus reactivation from latency. *J. Virol.* **80**(1), 192–200. <https://doi.org/10.1128/JVI.80.1.192-200.2006> (2006).
46. Dutia, B. M., Clarke, C. J., Allen, D. J. & Nash, A. A. Pathological changes in the spleens of gamma interferon receptor-deficient mice infected with murine gammaherpesvirus: A role for CD8 T cells. *J. Virol.* **71**(6), 4278–4283 (1997).
47. Tripp, R. A. *et al.* Pathogenesis of an infectious mononucleosis-like disease induced by a murine γ -herpesvirus: Role for a viral superantigen? *J. Exp. Med.* **185**(9), 1641–1650 (1997).
48. Hardy, C. L. *et al.* Factors controlling levels of CD8+ T-cell lymphocytosis associated with murine gamma-herpesvirus infection. *Viral Immunol.* **14**(4), 391–402. <https://doi.org/10.1089/08828240152716637> (2001).
49. Evans, A. G. *et al.* A gammaherpesvirus-secreted activator of Vbeta4+ CD8+ T cells regulates chronic infection and immunopathology. *J. Exp. Med.* **205**(3), 669–684. <https://doi.org/10.1084/jem.20071135> (2008).
50. Stevenson, P. G., Belz, G. T., Altman, J. D. & Doherty, P. C. Changing patterns of dominance in the CD8+ T cell response during acute and persistent murine gamma-herpesvirus infection. *Eur. J. Immunol.* **29**(4), 1059–1067. [https://doi.org/10.1002/\(SICI\)1521-4141\(199904\)29:04%3c1059::AID-IMMU1059%3e3.0.CO;2-L](https://doi.org/10.1002/(SICI)1521-4141(199904)29:04%3c1059::AID-IMMU1059%3e3.0.CO;2-L) (1999).
51. Barton, E. S., Rajkarnikar, S., Langston, P. K., Price, M. J. & Grayson, J. M. Gammaherpesvirus latency differentially impacts the generation of primary versus secondary memory CD8+ T cells during subsequent infection. *J. Virol.* **88**(21), 12740–12751. <https://doi.org/10.1128/JVI.02106-14> (2014).
52. Jacobsen, H. & Klein, S. L. Sex differences in immunity to viral infections. *Front Immunol.* **12**, 3483. <https://doi.org/10.3389/fimmu.2021.720952> (2021).
53. Ricker, E. *et al.* Altered function and differentiation of age-associated B cells contribute to the female bias in lupus mice. *Nat. Commun.* **12**(1), 4813. <https://doi.org/10.1038/s41467-021-25102-8> (2021).
54. Bussey, K. A. *et al.* Endosomal toll-like receptors 7 and 9 cooperate in detection of murine gammaherpesvirus 68 infection. *J. Virol.* **93**(3), e01173–e01218. <https://doi.org/10.1128/JVI.01173-18> (2019).

55. Krug, L. T., Collins, C. M., Gargano, L. M. & Speck, S. H. NF-kappaB p50 plays distinct roles in the establishment and control of murine gammaherpesvirus 68 latency. *J. Virol.* **83**(10), 4732–4748. <https://doi.org/10.1128/JVI.00111-09> (2009).
56. Rubtsova, K. *et al.* B cells expressing the transcription factor T-bet drive lupus-like autoimmunity. *J. Clin. Investig.* **127**(4), 1392–1404. <https://doi.org/10.1172/JCI91250> (2017).
57. Vockerodt, M. *et al.* The Epstein-Barr virus and the pathogenesis of lymphoma. *J. Pathol.* **235**(2), 312–322. <https://doi.org/10.1002/path.4459> (2015).
58. Shikova, E. *et al.* Cytomegalovirus, Epstein-Barr virus, and human herpesvirus-6 infections in patients with myalgic encephalomyelitis/chronic fatigue syndrome. *J. Med. Virol.* <https://doi.org/10.1002/jmv.25744> (2020).
59. Tsuge, I., Morishima, T., Kimura, H., Kuzushima, K. & Matsuoka, H. Impaired cytotoxic T lymphocyte response to Epstein-Barr virus-infected NK cells in patients with severe chronic active EBV infection. *J. Med. Virol.* **64**(2), 141–148. <https://doi.org/10.1002/jmv.1029> (2001).
60. Abernathy, E. *et al.* Gammaherpesviral gene expression and virion composition are broadly controlled by accelerated mRNA degradation. *PLoS Pathog.* **10**(1), e1003882. <https://doi.org/10.1371/journal.ppat.1003882> (2014).
61. Welsh, R. M. & Seedhom, M. O. LCMV: Propagation, quantitation, and storage. *Curr. Protoc. Microbiol.* <https://doi.org/10.1002/9780471729259.mc15a01s8> (2008).
62. Walter, D. L. *et al.* Coxsackievirus B4 exposure results in variable pattern recognition response in the kidneys of female non-obese diabetic mice before establishment of diabetes. *Viral Immunol.* **33**(7), 494–506. <https://doi.org/10.1089/vim.2019.0188> (2020).

Acknowledgements

The following reagent was obtained through the NIH Tetramer Core Facility: class I p79 tetramer. The authors thank the UBC LSI Flow Cytometry Core Facility and the UBC Modified Barrier Facility for their assistance and Martin Richer for the helpful feedback on the manuscript.

Author contributions

I.C.M. and M.S.H. conceived and designed the experiments; I.C.M. and I.S. conducted the experiments; I.C.M. and M.S.H. analyzed the results and wrote the manuscript.

Funding

The funding was provided by Canadian Institutes of Health Research.

Competing interests

The authors declare no competing interests.

Additional information

Supplementary Information The online version contains supplementary material available at <https://doi.org/10.1038/s41598-022-25543-1>.

Correspondence and requests for materials should be addressed to M.S.H.

Reprints and permissions information is available at www.nature.com/reprints.

Publisher's note Springer Nature remains neutral with regard to jurisdictional claims in published maps and institutional affiliations.



Open Access This article is licensed under a Creative Commons Attribution 4.0 International License, which permits use, sharing, adaptation, distribution and reproduction in any medium or format, as long as you give appropriate credit to the original author(s) and the source, provide a link to the Creative Commons licence, and indicate if changes were made. The images or other third party material in this article are included in the article's Creative Commons licence, unless indicated otherwise in a credit line to the material. If material is not included in the article's Creative Commons licence and your intended use is not permitted by statutory regulation or exceeds the permitted use, you will need to obtain permission directly from the copyright holder. To view a copy of this licence, visit <http://creativecommons.org/licenses/by/4.0/>.

© The Author(s) 2022